Available online at www.sciencedirect.com
SCIENCE DIRECT®
Journal of Catalysis 225 (2004) 105–115
JOURNAL OF CATALYSIS
www.elsevier.com/locate/jcat

Relations between structure and catalytic activity of Ce–In-ZSM-5 catalysts for the selective reduction of NO by methane II. Interplay between the CeO_2 promoter and different indium sites

T. Sowade,[a,1] T. Liese,[a,2] C. Schmidt,[a,3] F.-W. Schütze,[b,4] X. Yu,[a] H. Berndt,[b] and W. Grünert [a,*]

[a] *Lehrstuhl für Technische Chemie, Ruhr-Universität Bochum, D-44780 Bochum, Germany*
[b] *Institut für Angewandte Chemie Berlin-Adlershof, Richard-Willstätter-Straße 12, D-12489 Berlin, Germany*

Received 26 November 2003; revised 3 March 2004; accepted 5 March 2004

Available online 30 April 2004

Abstract

The promotion of In-ZSM-5 catalysts for the selective catalytic reduction of NO by methane by CeO_2 has been investigated by a combination of physicochemical techniques (XPS, EXAFS, TPR, XRD, FTIR) and reaction studies, in particular under variation of the activation conditions. CeO_2 is a highly effective promoter for In-ZSM-5 in dry feed (e.g., $X(\mathrm{NO}) > 70\%$ at 100,000 h^{-1} between 723 and 773 K with 1000 ppm NO, 1000 ppm CH_4, and 2% O_2) whereas in moist feed, the promotional effect is pronounced only at high temperatures. The role of CeO_2 in the reaction mechanism is to provide a sufficient NO_2 supply on the basis of its high NO oxidation activity. Under catalytic conditions, CeO_2 undergoes interaction with the zeolite component, which stabilizes part of the Ce ions in the +3 state in an oxidative atmosphere while the majority of Ce ions remain in the CeO_2 lattice. This effect does not appear to be constitutive for the catalytic function of the CeO_2 promoter. In-ZSM-5 catalysts with different active site structures exhibit different responses to promotion by ceria. Intrazeolite indium oxo species, which are often considered the most important active sites in In-ZSM-5 SCR catalysts, are not among the most favorable cases upon promotion with CeO_2. Intense promotional effects are found with sites that catalyze unselective methane oxidation in the absence of CeO_2 (intrazeolite InO_xCl_y species, extrazeolite In_2O_3 aggregates, probably active at the borderline with the zeolite). Ternary mechanical mixtures of CeO_2, $In(OH)_3$, and NH_4-ZSM-5 also exhibit high SCR activities provided that activation is performed in a nonoxidizing atmosphere. TPR, FTIR, XRD data, and results of experiments with separate activation of mixture components suggest that the favorable performance of these mixtures arises from extrazeolite indium sites, which are probably at the borderline between In_2O_3 aggregates and external zeolite surface and are possibly engaged in In–O–Si and In–O–Al bridges.

Keywords: SCR; Methane; CeO_2; In-ZSM-5; Active sites; XPS; EXAFS

1. Introduction

The world-wide interest in the selective catalytic reduction of nitric oxides by hydrocarbons (HC-SCR) [1–4] has inspired a great deal of work on the structural characterization of redox zeolites, which are active catalysts for HC-SCR. These studies have revealed an unexpected complexity in the site structure of redox zeolites. It has been found, for instance, that the redox activity of transition-metal cations (Cu^{n+}, Co^{n+}) depends on their location even in zeolites that do not possess hidden sites (ZSM-5, Beta, ferrierite [5,6]) and that aggregated structures bearing extralattice oxygen may play a prominent role in some catalytic systems, e.g., highly (or over)exchanged Cu-ZSM-5 and Fe-ZSM-5 [7–12]. The details, however, are often controversial. Thus, many groups assume a deciding role of dimeric structures in Cu-ZSM-5 and Fe-ZSM-5 [7,8,10,11,13], while it has been also argued that a multiplicity of sites including monomeric and oligomeric clusters may be responsible for the catalytic properties observed [9,12,14,15].

* Corresponding author. Fax: +49 234 321 4115.
E-mail address: w.gruenert@techem.ruhr-uni-bochum.de (W. Grünert).
[1] Present address: Sachtleben Chemie GmbH, 47198 Duisburg, Germany.
[2] Present address: ABB Lummus Global, Wiesbaden, Germany.
[3] Present address: Continental AG, Hannover, Germany.
[4] Present address: Umicore AG & Co. KG, Automotive Catalysts, D-63403 Hanau-Wolfgang, Germany.

0021-9517/$ – see front matter
doi:10.1016/j.jcat.2004.03.026

Indium-modified zeolites belong to the more popular catalysts for HC-SCR because they are able to activate the relatively inert methane molecule and to use it with considerable efficiency [16–21]. It has been found that these catalysts can be very effectively promoted with noble metals, which support the formation of the NO_2 intermediate insufficiently provided by the basic indium–zeolite system [22–24]. We have recently reported that (extrazeolite) CeO_2 has a similar effect, yielding catalysts with attractive activities for the SCR with methane and short alkane reductants, and a remarkable poisoning resistance to water, however, only at $T \geqslant 800$ K [25–27]. InO^+ ions on cation positions have been proposed to be the active sites in (promoted) In-ZSM-5 catalysts [17,18,22,28].

In our laboratory, the preparation, structure, and catalytic behavior of the basic In-ZSM-5 system have been investigated in some detail [21,29]. A combined XPS and EXAFS study [29] found that the coordination of intrazeolite indium species depends on the pH value of the exchange solution and that exclusively intrazeolite species are obtained only at low pH value and in minor quantities. Preparation at near-neutral pH value is accompanied by the precipitation of hydroxide species, which are transformed into aggregates with In_2O_3 short-range order upon calcination. The In–zeolite system is complicated by a significant tendency of extrazeolite In(III) species to migrate into intrazeolite locations under reductive conditions ("reductive solid-state ion exchange, RSSIE" [30]) or even under thermal evacuation ("autoreductive solid-state ion exchange" [31]). This can be used deliberately to produce intrazeolite indium species in large quantities by high-temperature reduction of precipitated or admixed In_2O_3 (e.g., Refs. [27,32], with In-MOR]), but it complicates any attempt to prepare model catalysts with exclusively extrazeolite indium oxide species. The intrazeolite indium species obtained by RSSIE, which are easily detected by a low-temperature peak during temperature-programmed reduction in hydrogen, are not necessarily mononuclear. Combined XPS, EXAFS, and IR studies suggested that intrazeolite oligomeric aggregates (possibly oligomeric cations) may have been also formed [29].

Alternative routes to intrazeolite indium species in appreciable quantities involve the use of $InCl_3$ (solid-state ion exchange, sublimation, and transport reaction—the latter differing from sublimation by lower temperatures and long residence times [21,29]). It has been found, however, that the In–Cl bond is rather stable under hydrolysis and calcination conditions, and its stability increases with the indium amount introduced. Therefore, chlorine remains in the indium coordination sphere even after washing and calcination except in samples with very low indium content [21,29].

On the basis of this knowledge, the SCR activity of intra- and extrazeolite indium species was described in part I of this contribution [21]. It was found that intrazeolite indium oxo species are, indeed, active sites for this reaction, but their catalytic properties (NO conversion–temperature profile) differ with differing indium coordination sphere. Extrazeolite indium species contribute unselective methane activation, i.e., total oxidation activity. The SCR activity of partially chlorided intrazeolite indium species is very poor, although they also exhibit a significant total oxidation activity for methane. Mechanical mixtures of $In(OH)_3$ and NH_4-ZSM-5, which were calcined in He prior to catalysis, provided SCR activities comparable to those of materials obtained by exchange or precipitation of indium. In these samples of comparable activity, the amount of intrazeolite indium species detected by TPR differed strongly.

In the present paper, the role of the CeO_2 promoter, its modification under conditions of activation and catalysis, and its interplay with the various indium sites encountered in In-ZSM-5 systems is described. It is demonstrated that the responses of these indium species to promotion are very different. The strongest promotion effect is achieved with sites that activate methane unselectively in the absence of NO_2—intrazeolite InO_xCl_y sites and a minority indium oxide site that has not yet been unequivocally identified. We believe the latter to be located at the boundary between extrazeolite In_2O_3 aggregates and the external zeolite surface.

2. Experimental

2.1. Materials

The ZSM-5 zeolite employed was provided by Alsi Penta (NH_4-ZSM-5, "SM 27", $Si/Al \approx 14$). Indium was applied in aqueous solutions of $In(NO_3)_3$ (Alfa Aesar, 99.99%) or as $InCl_3$ (ChemPUR, 99.99%). Despite its hygroscopicity, the latter was used without particular protection from the ambient atmosphere except if stated otherwise. $In(OH)_3$ was obtained from an $In(NO_3)_3$ solution by precipitation with aqueous ammonia (25%). The precipitate was washed in water and dried at 395 K. The CeO_2 employed was a high-surface-area material provided by Rhodia Co. (France), with a BET surface area of 190 m^2/g, which decreased to 90 m^2/g after 8 h calcination in stagnant air at 873 K.

The preparation of the basic In-ZSM-5 catalysts was described in detail in [21,29]. The samples used in the present study were prepared by ion exchange at different (initial) pH values, by precipitation, and by solid-state ion exchange of H-ZSM-5 with $InCl_3$. For ion exchange, a total of 5 g of NH_4-ZSM-5 was suspended in 400 ml of an $In(NO_3)_3$ solution (13 mmol/liter) and stirred overnight at room temperature. The initial pH of the $In(NO_3)_3$ solution was set to 6, 2.5, or 1.5 by adding HNO_3, or it was left at its natural value, which is approximately 6.5. After filtration, the exchange was repeated twice. Subsequently, the material was washed with water and dried at 393 K. These samples are designated by **IE**-6, **IE**-2.5, **IE**-1.5. For precipitation, a total of 2 g of H-ZSM-5 was suspended in 100 ml of a $In(NO_3)_3$ solution containing the desired amount of indium, and the precipitation was performed by adding 20 ml aqueous ammonia

Table 1
Explanation of sample designations

Code	Preparation	wt% In (Ce)
IE-6	Aqueous ion exchange, initial pH 6	In: 1.1
IE-2.5	Aqueous ion exchange, initial pH between 2 and 3	In: 0.25
IE-1.5	Aqueous ion exchange, initial pH between 1 and 2	In: 0.17
P	NH_4-ZSM-5 suspended in indium nitrate solution, immediate precipitation with ammonia	In: 7
P(H)	As **P**, but with H-ZSM-5	In: 7
SSIE(1)	Mixing $InCl_3$ with H-ZSM-5, heating in vacuo	In: 1.0
SSIE(3)	Mixing $InCl_3$ with H-ZSM-5, heating in vacuo	3.2
SSIE(4)	Mixing $InCl_3$ with H-ZSM-5, heating in vacuo	4.4
$\mathbf{MM}_{N,Hy}$	NH_4-ZSM-5 and $In(OH)_3$ ground together in a mortar and pelletized (= $\mathbf{MM}_{N,Hy}$(C))	In: 7
	Versions for comparative study:	In: 7
	$\mathbf{MM}_{N,Hy}$(A): NH_4-ZSM-5 pelletized, $In(OH)_3$ pelletized, pellets mixed, mixture activated at 873 K in He	
	$\mathbf{MM}_{N,Hy}$(B): activated mixture $\mathbf{MM}_{N,Hy}$(A), ground together and repelletized before new activation (873 K, He)	
	$\mathbf{MM}_{N,Hy}$(C): NH_4-ZSM-5 and $In(OH)_3$ ground together in a mortar and pelletized (= $\mathbf{MM}_{N,Hy}$)	
$\mathbf{MM}_{H,Hy}$	H-ZSM-5 and $In(OH)_3$ ground together in a mortar and pelletized	
Precipitates		
In first	**P**(H) suspended in cerium nitrate solution, immediate precipitation with ammonia	In: 7, Ce: 9
Together	H-ZSM-5 suspended in solution of cerium and indium nitrates, immediate precipitation with ammonia	In: 7, Ce: 9
Ce first	H-ZSM-5 suspended in cerium solution nitrate, immediate precipitation with ammonia, dried product suspended in indium nitrate solution, immediate precipitation with ammonia	In: 7, Ce: 9

(25%). The samples were washed with water, dried at 393 K, and calcined in helium at 873 K (heating protocol—2 K/min to 393 K, 5 K/min to 873 K, 2 h isothermal). These samples are referred to as **P**. For solid-state ion exchange, $InCl_3$ was intimately mixed with dehydrated H-ZSM-5, transferred to a vacuum vessel, and evacuated under a temperature regime including a 5 K/min ramp from room temperature to 873 K and a 2-h isothermal period at this temperature. The samples, which are designated **SSIE**, were studied after cooling and exposure to air. The designations are summarized in Table 1, where the indium contents of the samples as determined from X-ray absorption spectra [29] are given as well.

In most cases, the CeO_2 promoter was added to the basic In-ZSM-5 by grinding both components together. The amount was chosen to yield 9 wt% Ce in the final catalyst. In preliminary experiments, precipitation of the Ce component (9 wt% Ce) onto the external surface was also tested. The precipitation of cerium hydroxide was performed analogously to that of indium hydroxide; i.e., 2 g of H-ZSM-5 (or of In-ZSM-5 previously made by precipitation) was suspended in 100 ml of a $Ce(NO_3)_3$ solution containing the desired amount of cerium, the precipitation was performed by adding 20 ml aqueous ammonia (25%), and the preparation was completed by the drying and calcination steps already described. As indicated above, the sequence of indium and cerium precipitation was varied, and a coprecipitation was performed as well.

Mechanical mixtures were prepared by grinding the zeolite (H or NH_4 form) together with an indium source (usually $In(OH)_3$) and CeO_2. It is important to note that the catalysts obtained from these mixtures by standard pelletizing (compacting, crushing, and sieving) were usually thermally activated in helium before the catalytic runs because such activation may be expected to induce reductive solid-state ion exchange on the basis of literature results [33]. As in part I [21], a segregated mixture ($In(OH)_3$ and NH_4-ZSM-5 pelletized separately and mixed in pelletized form, CeO_2 added by a shaking procedure, labeled A) was compared with a mixture obtained by grinding and repelletizing the segregated binary mixture *after* thermal activation in inert gas and adding CeO_2 (type B). The results will be referred to those of the standard mixture (made by jointly pelletizing $In(OH)_3$ with NH_4-ZSM-5 and adding CeO_2), which will be labeled C. The mechanical mixtures will be labeled **MM**, with indices indicating the form of the ZSM-5 used and the indium source (Hy—hydroxide), e.g., $\mathbf{MM}_{N,Hy}$(B) (cf. Table 1). In addition, an extended set of mixtures of particular preparation was used to study the influence of certain activation steps on the final activity of the mixtures. In these preparations, two of the components were initially ground together and subjected to an activation treatment before the third component was added. The details of these preparations are given below together with the results. In the physical mixtures, indium and cerium contents were 7 and 9 wt% if not stated otherwise.

In many parts of the paper, reference is made to calcination pretreatments of samples in synthetic air or in He. Such treatments are always analogous to the thermal activation mentioned above, i.e., a 5 K/min ramp to 873 K and a 2-h isothermal period at this temperature.

2.2. Methods

XP spectra were measured with a Leybold LH 10 spectrometer equipped with an EA 10/100 multichannel detector (Specs), using Mg-K_α excitation (1253.6 eV, 10 kV *

20 mA). The samples were studied after contact with the atmosphere. The binding-energy (BE) scale was referenced to the Si($2p$) line as an internal standard (Si($2p$) = 103.0 V).

X-ray absorption spectra (Ce L_3 edge at 5.724 keV) in transmission mode were collected at Hasylab E4 station (Hamburg) using a Si(311) double crystal monochromator (higher harmonics excluded by detuning to 70% maximum intensity). Samples were measured at liquid nitrogen temperature (77 K); the spectrum of a Ce metal foil was recorded at the same time (between the second and a third ionization chamber) for energy calibration. The catalysts were diluted with polyethylene, pressed into disks of suitable thickness, and stored in ambient atmosphere before the measurements. Data reduction of experimental XAFS was performed with standard procedures as described, e.g., in [34,35], which are implemented in the software package WinXAS2.0 [36]. They include pre-edge background subtraction and XANES normalization (linear polynomial for the pre-edge region, third-order polynomial for post-edge region, smooth atomic background ($\mu_0(k)$) via cubic splines). The radial distribution function FT[$k^3\chi(k)$] was evaluated by Fourier transformation into the R space of the k^3-weighted experimental function $\chi(k) = (\mu(k) - \mu_0(k))/\mu_0(k)$ multiplied by a Bessel window.

Temperature-programmed reduction was carried out with a mixture containing 5.2 vol% H_2 in Ar (50 ml/min), with a 10 K/min temperature ramp between room temperature and 1073 K. The samples were studied after catalysis. Prior to TPR, they were calcined in air at 873 K. The hydrogen content of the effluent was measured by a catharometer.

2.3. Catalysis

As described in part I [21], the SCR of NO with methane was studied in a catalytic microflow reactor in the temperature range 873 to 523 K. If not stated otherwise, standard reaction conditions (1000 ppm NO, 1000 ppm methane, 2% O_2 in He, at 30,000 h^{-1}) were applied. The catalyst was employed in 250- to 350-μm particles, in beds of 0.65–0.70 g/ml bed density depending on the catalyst composition so that the GHSV of 30,000 h^{-1} resulted in $W/F \approx 0.08$ g s cm^3. Approximately 300 mg of catalyst (a bed volume of 0.44 ml) was initially heated in flowing He to 873 K at 5 K/min and kept at this temperature for 1 h. The feed mixture was then charged to the catalyst at a flow rate of 220 ml/min. After analysis of the reduction products, the next experimental temperature was established in a schedule with temperatures descending from the highest to the lowest value. Deviations from the standard conditions include the use of moist feed (2% H_2O) or increased GHSV (100,000 h^{-1}).

The products were analyzed by a combination of gas chromatography (O_2, N_2, CH_4), calibrated mass spectrometry (NO, CH_4, NO_2), and calibrated nondispersive IR photometry (CO, CO_2, N_2O). In this analysis scheme, NO_2 is detected with low sensitivity because of its unfavorable fragmentation behavior in the mass spectrometer. However, on the basis of test experiments with a different analysis scheme including UV analysis for NO_2 and nondispersive IR-photometric analysis for NO, it was concluded that NO_2 was not formed in significant amounts under the reaction conditions employed. This is confirmed by C and N balances of typically 100 ± 5% obtained in the catalytic runs.

A possible influence of diffusion limitations (external diffusion, pore diffusion in pressed particles) has been excluded by standard tests with one of the most active catalysts employed [37]. This does not cover possible diffusion limitations on the scale of the zeolite crystals, which have been reported for HC-SCR with Co zeolites [38]. However, as the same zeolite material was used throughout the entire study, this does not affect the activity rankings observed: whereas the highest overall reaction rates might be significantly influenced by diffusion, lower rates measured under the same conditions will be influenced to a smaller extent, i.e., diffusion limitations may have attenuated differences but not reversed rankings.

3. Results and discussion

3.1. Catalytic behavior of CeO_2–In-ZSM-5 catalysts in the SCR with methane

In Fig. 1, typical activity data obtained with CeO_2–In-ZSM-5 catalysts of different preparation are presented. The black curves refer to the basic In-ZSM-5 system prepared by precipitation (**P**). Without promotion, it achieves a peak NO conversion of about 30% at 723 K. In the mixture with high-surface-area CeO_2, the peak conversion increases to > 90% achieved at temperatures between 723 and 773 K. The high activity of this system is illustrated by a measurement at 100,000 h^{-1}, where NO conversions > 70% were obtained in the same temperature range. In these somewhat short experimental series, no data for lower temperatures were measured, but experience with other CeO_2–In-ZSM-5 catalysts ([27]; see also below) suggests that the NO conversion would have strongly decreased to 30–50% at 673 K for 30,000 h^{-1}.

Figure 1 provides also information about the introduction of the promoter by precipitation (gray curves). Different precipitation sequences are compared with coprecipitation. It may be observed that the changes are not very pronounced, although a preference for the final precipitation of the ceria component is apparent. At the same time, precipitation of the Ce component is clearly inferior to the physical admixture of high-surface-area CeO_2. Although a stringent interpretation of the trends seen with the precipitate catalyst would require a detailed characterization of the precipitates, the results imply that a high ceria surface is crucial for good catalyst performance. Indeed, much lower SCR activities were found when In-ZSM-5 was promoted with a home-made CeO_2 of lower surface area (ca. 60 m^2/g [39]).

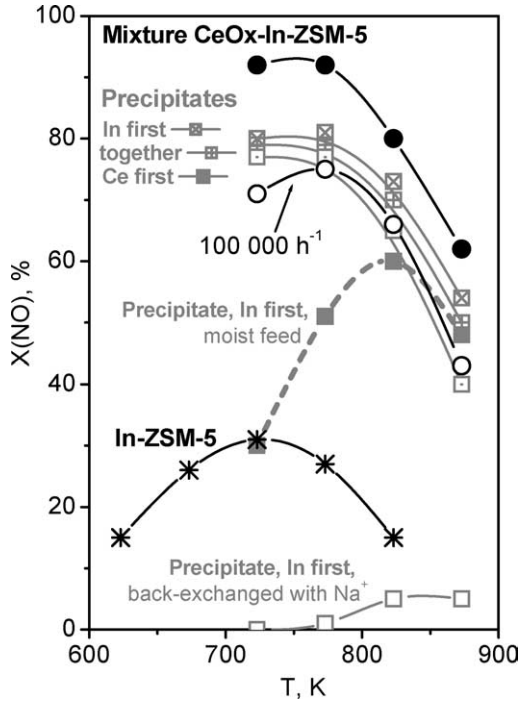

Fig. 1. SCR of NO with methane over In-ZSM-5 catalysts promoted with CeO_2. 1000 ppm NO, 1000 ppm methane, 2% O_2 in He at 30,000 h^{-1}. Black curves—mixtures of In-ZSM-5 with high-surface-area CeO_2; gray curves—CeO_2 introduced via precipitation. ∗, Unpromoted In-ZSM-5 (sample **P** (see Table 1)); ●, **P** physically mixed with high-surface-area CeO_2 (9 wt% Ce); ○, same as ● but at 100,000 h^{-1}; ⊠, precipitate, In first (see Table 1); ■, the same, 2 vol% H_2O added to feed; □, precipitate, In first, zeolite protons back-exchanged with 1 M $NaNO_3$ solution; ⊞, precipitate, together; ⊡, precipitate, Ce first.

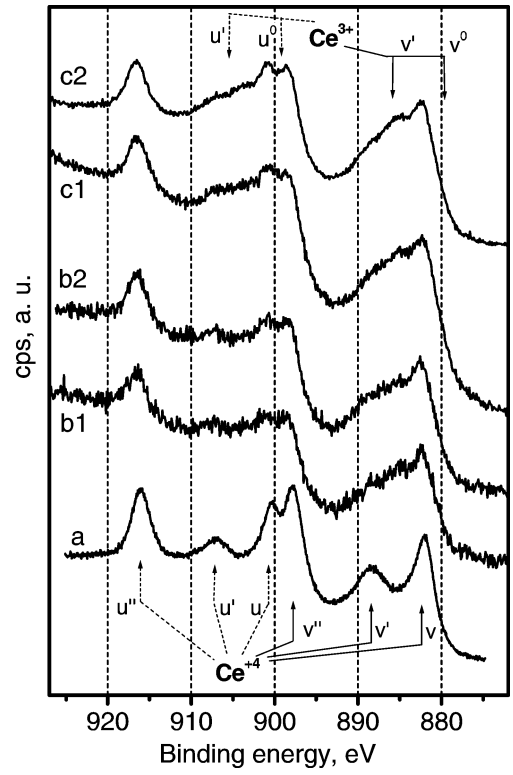

Fig. 2. Ce 3d XP spectra of the CeO_2 promoter in CeO_2–In-ZSM-5 catalysts after thermal treatments. (a) CeO_2 reference; (b) $\mathbf{MM}_{N,Hy}$ mixed with CeO_2; (b1) after use in SCR reaction; (b2) after activation in 20% O_2/He at 873 K; (c) NH_4-ZSM-5 mixed with CeO_2; (c1) after activation in He at 873 K; (c2) after activation in 20% O_2/He at 873 K.

In addition, Fig. 1 gives data about the influence of moisture and of the poisoning of acidic protons by Na^+. The addition of 2 vol% H_2O to the feed drastically decreases the NO conversion of **P** promoted with ceria by precipitation, although the residual activity is much higher than that for the unpromoted catalyst ($X_{NO}(max) < 12\%$ [21]). A back-exchange of protons with Na^+ (by stirring in a 1 mol/liter $NaNO_3$ solution) completely quenches all activity as with the unpromoted system [21].

3.2. Physicochemical characterization of the Ce component

The structural information available for the basic In-ZSM-5 system, which was published in [21,29], is summarized in the introduction. The CeO_2 was added with the intention to have it present as a high-surface-area extrazeolite component, but the thermal stress to which the catalysts are subjected during thermal pretreatment and catalysis may cause the CeO_2 to interact with the zeolite and the indium component. To elucidate relevant structural changes in the ceria component during calcination or catalysis, XPS and EXAFS measurements were performed with selected samples.

The effect of such thermal stress on the Ce 3d XPS signal of the CeO_2 promoter in binary mixtures with NH_4-ZSM-5 and in the full mixture with NH_4-ZSM-5 and $In(OH)_3$ ($\mathbf{MM}_{N,Hy}$ + CeO_2) is shown in Fig. 2. The CeO_2 is in all cases the high-surface-area material described in the experimental part, the spectrum of which is included as a reference (a). The treatments were activation in He at 873 K with subsequent use in catalysis (b1; for results see below, e.g., Figs. 7, 8), activation in 20% O_2/He at 873 K (b2, c2), activation in He at 873 K (c1), in all cases followed by a re-oxidation in air at 873 K. Ce 3d XP spectra are very complex due to a rich satellite structure, which is labeled in the figure (v, v′, v″ and u, u′, u″ for Ce^{4+} ($3d_{5/2}$ and $3d_{3/2}$, respectively)—v^0, v′ and u^0, u′ for Ce^{3+}). Quantitative analysis of the oxidation states requires a difficult peak-fitting analysis [40], but qualitatively, it is quite clear that a significant amount of Ce^{3+} has been formed in all cases. Given the final reoxidation of all samples, this Ce^{3+} indicates that part of the Ce ions have undergone interaction with the zeolite component: Whereas Ce^{3+} would not survive an oxidative treatment on the surface of CeO_2, it is known from the literature that interactions of CeO_2 with a support, e.g., Al_2O_3, can stabilize the +3 oxidation state [41]. It is remarkable that this interaction between NH_4-ZSM-5 and CeO_2 took place irrespective of the calcination atmosphere (compare spectra c1 and c2).

However, the EXAFS spectra in Fig. 3 (k^3-weighted Fourier transforms of the absolute part) show that the ma-

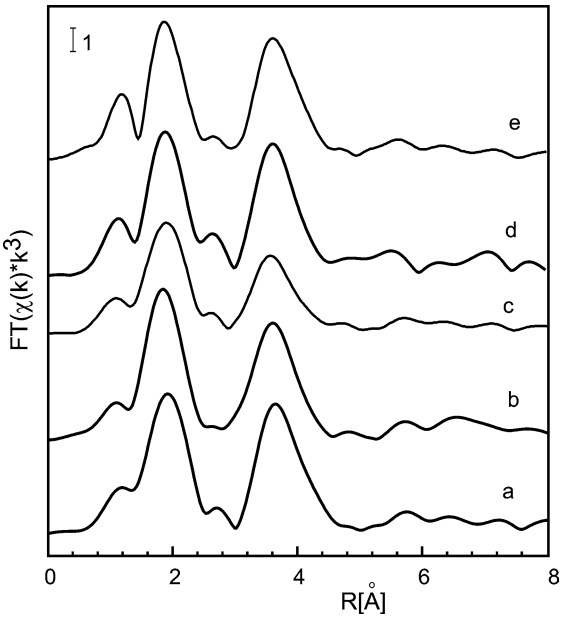

Fig. 3. EXFAS spectra (k^3-weighted absolute value of Fourier transform) of CeO_2–In-ZSM-5 catalysts. Curves: (a) CeO_2 reference; (b) CeO_2 precipitated on H-ZSM-5 (9 wt% Ce), reference; (c) precipitate, together; (d) precipitate, In first (see Table 1); (e) precipitate, Ce first. All samples activated in 20% O_2/N_2 at 873 K.

jority of the Ce ions remain in CeO_2 short-range order. In this figure, Ce L_3 spectra of catalysts prepared by precipitation of the In and the Ce component in different order (for catalytic data see Fig. 1; EXAFS measured after calcination in 20% O_2/N_2) are compared with that of CeO_2. Because in these precipitate catalysts, the ceria and the zeolite component are closer to each other than in the mechanical mixtures, the Ce ions should have the highest tendency to interact with the surface of the zeolite or even enter the pores. However, the spectra of the precipitate catalysts are very close to that of CeO_2; i.e., the majority of the Ce ions remain in CeO_2 aggregates. The lower intensity of the scattering features in the coprecipitated catalyst most likely arises from a higher disorder from intense mixing with aggregates of In_2O_3 structure, which are detected at the In *K*-edge with these samples [42]. Beyond this coprecipitated catalyst, interactions between the In and the Ce component could not be detected. The XANES region of the Ce L_3 XAFS spectra did not indicate the presence of significant quantities of Ce^{3+}. This shows that the Ce^{3+} species found by XPS are a minority state, most likely confined to the external region of the zeolite crystals. There they can be sensitively detected by XPS while most of the Ce^{4+} ions in the bulk of CeO_2 particles much larger than the photoelectron escape depth will not be seen.

3.3. The role of the CeO_2

The analogy of the present catalysts with the noble-metal-promoted In zeolites suggests that the role of ceria is to provide a rich supply of NO_2, which is a likely reaction intermediate. Indeed, high NO oxidation activity of CeO_2 was

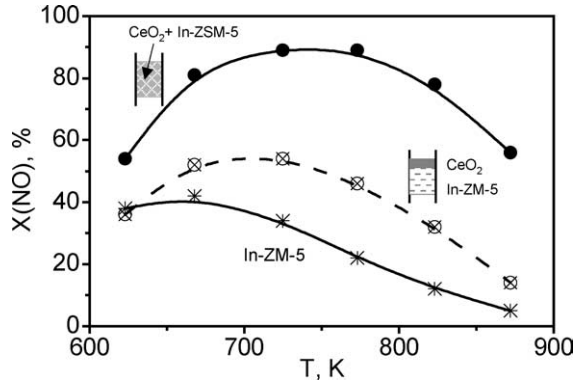

Fig. 4. Influence of separation between In-ZSM-5 and CeO_2 on the promotional effect. 1000 ppm NO, 1000 ppm methane, 2% O_2 in He, 30,000 h^{-1}. "In-ZSM-5"—**IE**-6; ∗, unpromoted In-ZSM-5; ⊗, CeO_2 in front of In-ZSM-5 (9 wt% Ce); ●, CeO_2 mixed with In-ZSM-5 (9 wt% Ce).

observed in earlier studies on binary CeO_2–H-ZSM-5 catalysts [43]. However, a different mechanism of bifunctional interaction was found to operate in CH_4-SCR over these indium-free materials where ceria appears to activate both methane and NO, releasing a short-lived intermediate containing both C and N for further chemistry into the acidic zeolite [43]. These alternatives can be easily distinguished by separating the CeO_2 from the basic (In-ZSM-5) catalyst into a preceding layer.

Figure 4 presents the outcome of this experiment. The unpromoted In-ZSM-5 is **IE**-6 here, the NO conversion-temperature curve of which differs from that of **P** (Fig. 1) and peaks at a conversion of ≈ 40%. Also with this **IE**-6, the addition of high-surface-area CeO_2 increases the peak NO conversion to ≈ 90%. On the other hand, a significant increase in the NO conversion is also seen when the CeO_2 layer is placed in front of the In-ZSM-5 bed. This indicates that a long-lived intermediate, most likely NO_2, is produced on the ceria surface. The promotional effect is smaller with the layered catalyst bed than with the mixture because in the former case, the NO/NO_2 equilibrium is approached only once (in the layer) irrespective of the amount of CeO_2 present. In the mixture, the NO oxidation always proceeds far from equilibrium because NO_2 is continuously transformed over the In-ZSM-5 component; hence, the higher NO oxidation activity of the high-surface-area ceria can be fully utilized. In summary, the mechanism of the bifunctional interaction differs from that found with CeO_2/H-ZSM-5 catalysts [43]. This does not mean that the latter is necessarily suppressed, but it renders only small contributions to the reaction rate, which is much higher over the indium-containing catalysts.

3.4. Promotion of different In sites with CeO_2

In part I of this study [21], a variety of In sites were discriminated in ZSM-5 catalysts prepared via different routes. Figures 5 and 6 describe the effect of the CeO_2 promoter

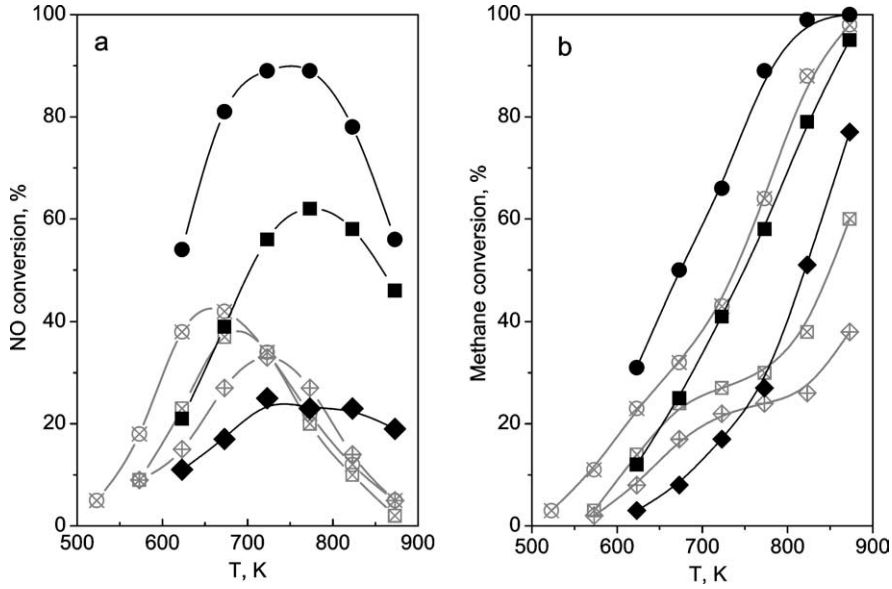

Fig. 5. Influence of physically admixed high-surface-area CeO_2 (9 wt% Ce) on the SCR activity of different In-ZSM-5 catalysts. 1000 ppm NO, 1000 ppm methane, 2% O_2 in He at 30,000 h^{-1}. (a) NO conversion; (b) methane conversion. ⊗, **IE**-6 (cf. Table 1); ●, **IE**-6 + CeO_2; ⊠, **IE**-2.5; ■, **IE**-2.5 + CeO_2; ⊕, **IE**-1.5; ◆, **IE**-1.5 + CeO_2.

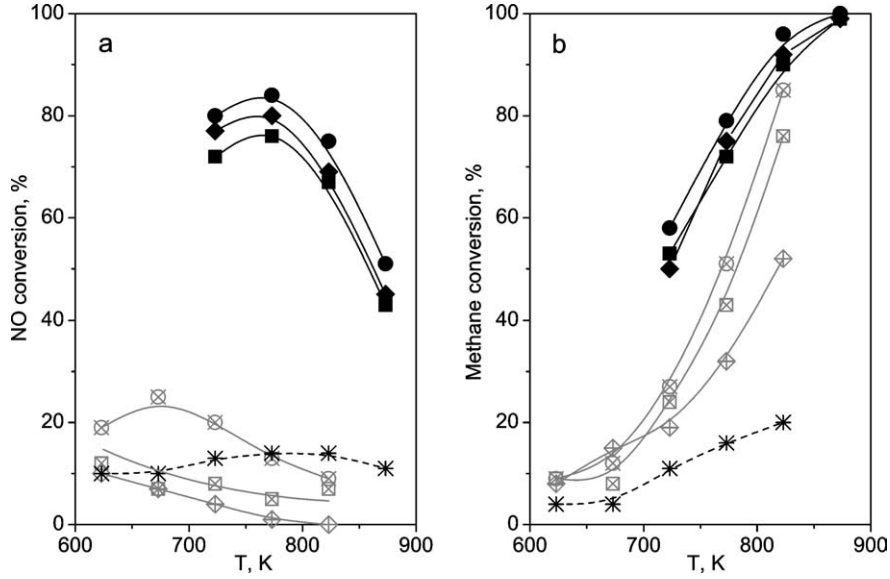

Fig. 6. Influence of physically admixed high-surface-area CeO_2 (9 wt% Ce) on the SCR activity of In-ZSM-5 catalysts with mixed InO_xCl_y coordination sphere around In (cf. [21,29]). 1000 ppm NO, 1000 ppm methane, 2% O_2 in He at 30,000 h^{-1}. (a) NO conversion; (b) methane conversion. ∗, Parent H-ZSM-5 (reference); ⊗, **SSIE**(1); ●, **SSIE**(1) + CeO_2; ⊠, **SSIE**(3); ■, **SSIE**(3) + CeO_2; ⊕, **SSIE**(4); ◆, **SSIE**(4) + CeO_2.

(i.e., of rich NO_2 supply) on the SCR over these sites. The effect varies dramatically when different indium oxo sites are compared (Fig. 5). Catalyst **IE**-6, which contains both intra- and extrazeolite In oxo species [29], is strongly promoted, as already seen in Fig. 4. An intermediate effect limited to higher temperature is seen with **IE**-2.5, in which exclusively intrazeolite In oxo species were detected, the average coordination sphere around which differed from that around the intrazeolite In sites in **IE**-6 [29]. Surprisingly, **IE**-1.5, for which a further change in the indium coordination sphere was suggested in [29], is not at all promoted by a rich NO_2 supply. Even the methane activation is somewhat suppressed at low temperatures (cf. Figs. 5a and b).

In part I [21], intrazeolite indium species containing chlorine in their coordination spheres (**SSIE**) were found to exhibit disappointing SCR activities despite a considerable capability of activating methane. Their response to promotion with CeO_2 is quite encouraging: even catalysts yielding NO conversions below those over the parent H-ZSM-5 are boosted to achieve peak NO conversions of 76–84% (Fig. 6).

From these results and that of **IE**-6 (Fig. 5), it appears that particular promotional effects are achieved with catalysts that exhibit high but unselective methane activation capability in the unpromoted version. This can be rationalized by two different explanations. The first one assumes that methane is always activated over In oxo sites, and at rich NO_2 supply the SCR reaction wins the competition for this species over the oxygen. Alternatively, an adsorption competition between CH_4 and NO_2 must be assumed for the In oxo sites, methane being both selectively and unselectively activated on indium oxo sites, but only selectively by adsorbed NO_2. The adverse effect of NO_2 on the methane activation over **IE**-1.5 cannot be explained by the first hypothesis, whereas it can be understood by assuming that the selective methane activation by adsorbed NO_2 is relatively slow on the indium oxo sites in **IE**-1.5. Thus, adsorbed NO_2 might block sites that would otherwise function via direct activation of methane by In oxo ions.

In summary, it appears that different indium sites yield different responses to promotion by CeO_2. The response of intrazeolite In oxo species is not necessarily favorable. It is not clear as yet which site supports the high activity of **IE**-6. In part I [21], the unselective methane activation capability of the unpromoted material was ascribed to sites at the borderline between zeolite and extrazeolite In_2O_3 aggregates. From this, it may be suggested that the particular favorable response of this material to a rich NO_2 supply is also due to these sites.

3.5. Activity and activation of physical mixtures

In part I of this study [21], it was reported that physical mixtures of $In(OH)_3$ and NH_4-ZSM-5 yield activities similar to those of samples prepared by ion exchange of precipitation provided that they had undergone thermal treatment in inert gas in a state where the indium and the zeolite component are in close proximity. In Fig. 7a, the response of such mixtures to promotion by CeO_2 is described. It can be seen that the catalytic behavior of mixture $\mathbf{MM}_{N,Hy}(A)$ made of separate pellets of NH_4-ZSM-5 and $In(OH)_3$ ("segregated mixture") is not much improved by the promoter. On the other hand, both the standard mixture $\mathbf{MM}_{N,Hy}(C)$ and mixture $\mathbf{MM}_{N,Hy}(B)$ obtained by crushing and repelletizing the activated $\mathbf{MM}_{N,Hy}(A)$ achieve excellent and nearly identical activities after promotion with ceria. Under an explanation pattern that assumes the sites responsible for the extra activity to be intrazeolite indium oxo species formed via reductive solid-state ion exchange, this result is unexpected because in mixture (B) the zeolite and the indium component were separated during evolution of the reductant NH_3. Obviously, the activation process that proceeds during the thermal treatment of the (B) pellets containing H-ZSM-5 and partially reduced In_2O_3 (from crushing and repelletizing the activated (A)) leads to a similar result.

Figure 7b displays TPR traces of these catalysts after use in catalysis. The patterns are similar to those of the unpromoted mixtures [21]; a contribution of the CeO_2 cannot be detected as earlier described in [26,27]. Mixture (A) is reduced in one asymmetric peak at 860 K, whereas this main peak shifts to somewhat lower temperatures with the remaining mixtures. A low-temperature peak that could be assigned to intrazeolite indium species (cf. reference trace of an ammonia-precipitated In–H-ZSM-5 after thermal treatment in He) cannot be clearly discerned. There is, however, a weak, strongly smeared out, low-temperature shoulder in the trace of mixtures (B) and (C). When the catalytic activity of the (promoted) reference sample **P**(H) is included, a correlation between the quantity of intrazeolite indium sites

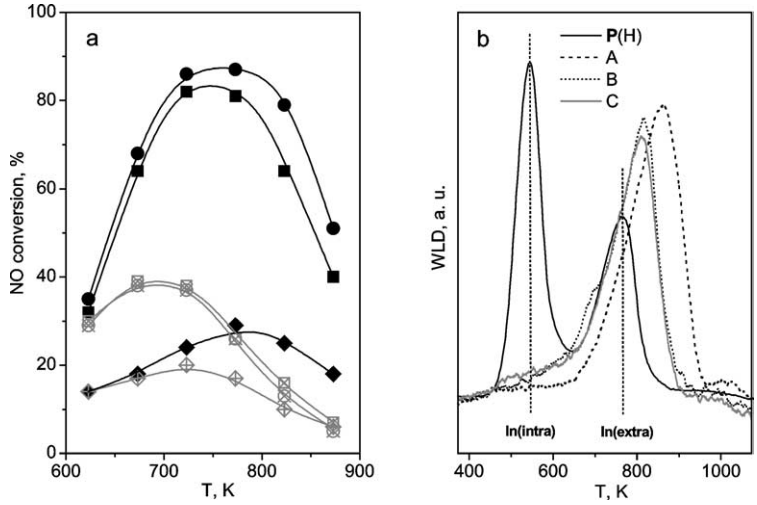

Fig. 7. SCR with physical mixtures between CeO_2, $In(OH)_3$, and NH_4-ZSM-5, influence of the separation between components on activity and location of indium species. 1000 ppm NO, 1000 ppm methane, 2% O_2 in He at 30,000 h^{-1}. (a) NO conversions; ◇, $\mathbf{MM}_{N,Hy}(A)$ (separate pellets of $In(OH)_3$ and NH_4-ZSM-5); ⟐, $\mathbf{MM}_{N,Hy}(A) + CeO_2$; ⊗, $\mathbf{MM}_{N,Hy}(B)$ ($\mathbf{MM}_{N,Hy}(A)$ activated in He at 873 K, subsequently crushed, repelletized, and again activated in He); ●, $\mathbf{MM}_{N,Hy}(B) + CeO_2$; ⊠, $\mathbf{MM}_{N,Hy}(C)$ ($In(OH)_3$ and NH_4-ZSM-5 pelletized together); ■, $\mathbf{MM}_{N,Hy}(C) + CeO_2$. (b) TPR traces, recorded after catalysis: ——, **P**(H), reference; – – –, $\mathbf{MM}_{N,Hy}(A) + CeO_2$; ···, $\mathbf{MM}_{N,Hy}(B) + CeO_2$; ——, $\mathbf{MM}_{N,Hy}(C) + CeO_2$.

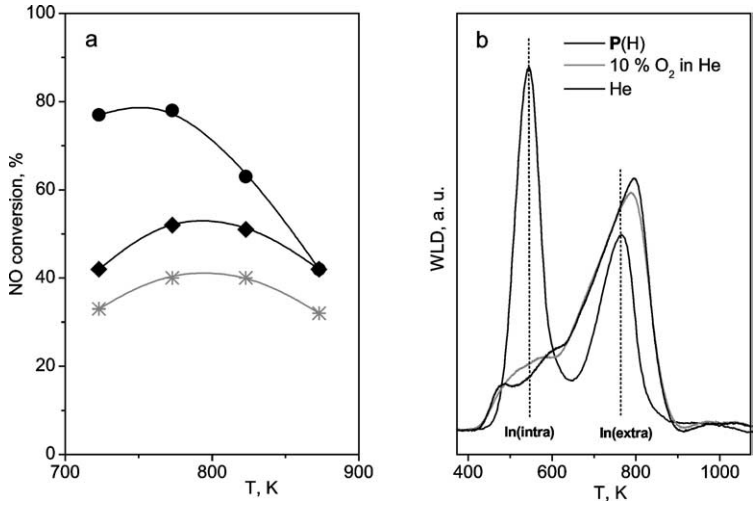

Fig. 8. SCR with physical mixtures between CeO_2, $In(OH)_3$, and ZSM-5, influence of the activation atmosphere on SCR activity and location of indium species. 1000 ppm NO, 1000 ppm methane, 2% O_2 in He at 30,000 h^{-1}. (a) NO conversions: black curves—$\mathbf{MM}_{N,Hy}(C) + CeO_2$; ●, activation in He; ◆, activation in 10% O_2/He; gray curve—$\mathbf{MM}_{H,Hy} + CeO_2$, activated in He. (b) TPR traces, recorded after catalysis: ——, **P**(H), reference, ——, $\mathbf{MM}_{N,Hy} + CeO_2$, activated in He; ——— , $\mathbf{MM}_{N,Hy} + CeO_2$, activated in 10% O_2/He.

and the SCR activity is impossible: almost the same NO conversion/temperature profiles are obtained with samples of widely varying amounts of intrazeolite indium species.

As mentioned above, the high activities reported so far are observed only when the physical mixtures are thermally activated in inert gas. Figure 8a shows a high activity for a mixture $\mathbf{MM}_{N,Hy} + CeO_2$ thermally treated in He, but activation of the same physical mixture in a oxidative atmosphere (10% O_2/He) is unfavorable. The lowest activity, however, was obtained when H-ZSM-5 was used instead of NH_4-ZSM-5 (i.e., $\mathbf{MM}_{H,Hy}$) even though the activation was performed in He. Clearly, the presence of a reducing agent during the thermal treatment is crucial for a favorable result. Figure 8b shows completely identical TPR traces of $\mathbf{MM}_{N,Hy}$ activated in 10% O_2/He or in He. It again becomes obvious that the pronounced activity difference between these catalyst states cannot be ascribed to a varying amount of intrazeolite indium oxo species.

The search for the sites responsible for the extra activity obtained by activation in inert gas must therefore focus on the extrazeolite indium oxide aggregates with In_2O_3 short-range order. At the same time, it has not yet been excluded that the effect originates from the ceria component which has been shown to undergo changes during activation and catalysis as well (cf. Fig. 3).

The latter hypothesis was examined in an experiment in which a physical mixture of $In(OH)_3$ and NH_4-ZSM-5 was first subjected to the standard thermal treatment in He while the final catalyst was calcined in 20% O_2/He under the same conditions after the CeO_2 promoter had bee added. The high NO conversions observed with this preparation (Fig. 9) despite the final oxidative calcination (compare with Fig. 8) proves that the active sites are formed in an interaction between the indium component and the zeolite. It shows at the same time that the extra activity does not arise

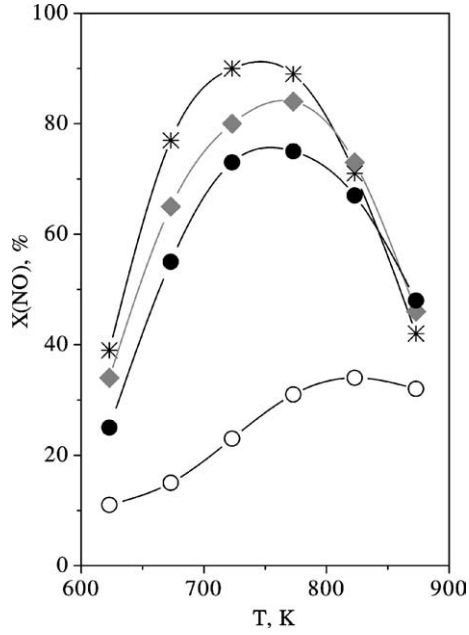

Fig. 9. NO conversions achieved with physical mixtures of the type $\mathbf{MM}_{N,Hy} + CeO_2$, with different activation sequence of components. 1000 ppm NO, 1000 ppm methane, 2% O_2 in He at 30,000 h^{-1}. ∗, {$In(OH)_3 + NH_4$-ZSM-5} activated in He, mixed with CeO_2, final activation in 20% O_2/He; ●, {$CeO_2 + NH_4$-ZSM-5} activated in He, mixed with $In(OH)_3$ activated in 8300 ppm NH_3/He, final activation in He; ○, the same as ●, but final activation in 20% O_2/He; ◆, CeO_2 reduced in H_2 (823 K, 2 h), mixed with $In(OH)_3$ and H-ZSM-5, final activation in He.

from defects on the surface of the extrazeolite In_2O_3 aggregates, which may have been formed during activation in the slightly reducing medium. Such defects should have been reoxidized during the final oxidative calcination. In accordance with this, the performance of a He-activated $\mathbf{MM}_{N,Hy}$ mixture ($X_{NO} = 76\%$ at 723 K) did not significantly deteriorate when the reductant methane or both methane and NO

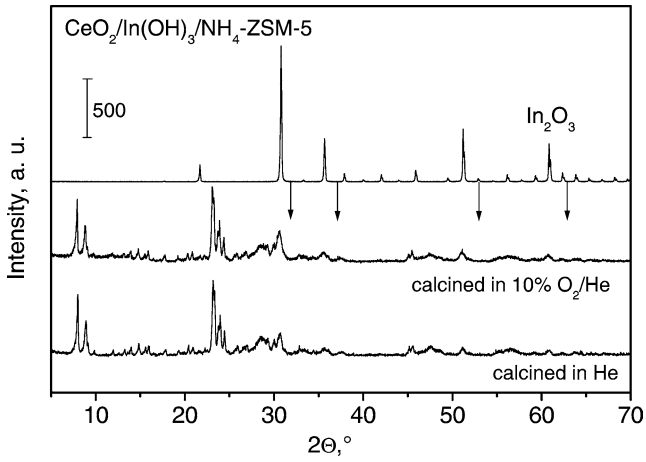

Fig. 10. X-ray diffractograms of In_2O_3 (reference), $\mathbf{MM}_{N,Hy}(C) + CeO_2$, activated in 10% O_2/He or in He.

were removed from the feed for 1 h. Obviously, the sites responsible for the extra activity are stable in an oxidative atmosphere. On this basis, a decisive role of the ceria component could be additionally disproved by an experiment in which a CeO_2/NH_4-ZSM-5 mixture thermally treated in He under the standard activation conditions and $In(OH)_3$ preactivated in 8300 ppm NH_3/He were mixed together to give the final catalyst. As shown in Fig. 9, this catalyst exhibited an appreciable SCR activity when subjected to the standard He activation, but showed poor performance when calcined in 20% O_2/He. Because the sites yielding the extra activity survive oxidative treatments once having been formed, they obviously do not arise from the interaction between CeO_2 and NH_4-ZSM-5.

Our attempts to provide direct evidence for the active sites under investigation failed. The IR spectra (OH region) of $\mathbf{MM}_{N,Hy}$ activated in 10% O_2/He and in He were virtually identical [41], in accordance with expectations given the low amount of intrazeolite indium species concluded from the TPR studies (Figs. 7, 8). In XRD, however, the In_2O_3 reflections of the mixture activated in He were significantly smaller than those in the oxidized sample (Fig. 10). This indicates that treatment in a slightly reducing atmosphere leads to smaller oxide particles than oxidative calcination, apparently with a higher amount of X-ray amorphous In oxide material. This difference may arise from an increased mobility of the indium in a slightly reducing atmosphere, which would lead to reductive solid-state ion exchange at full reductant supply.

On this basis, we assign the extra activity of mechanical CeO_2/$In(OH)_3$/NH_4-ZSM-5 mixtures activated in inert gas to indium sites at the border between indium oxide aggregates and zeolite (possibly engaged in In–O–Si or In–O–Al bridges). This assignment is in agreement with the observation that among In-ZSM-5 samples prepared by ion exchange, the one containing both intra- and extrazeolite indium oxo species (**IE**-6) is most effectively promoted by CeO_2 (Fig. 5). Such sites should be stable in an oxidative atmosphere, and their preferred formation under slightly reducing conditions may be explained by the mobility argument mentioned above. The details of the process leading to higher In_2O_3 dispersion, however, are still obscure. Thus, a mixture prepared from CeO_2 previously reduced in H_2 with H-ZSM-5 and $In(OH)_3$ also achieved peak NO conversions of 85% (cf. Fig. 9). Because effective storage of H_2 by ceria is unlikely, there is no reducing agent in the system but the oxygen vacancies left on the ceria by the reduction. Hence, an explanation for the successful activation would have to assume a solid-state reaction between the partially reduced ceria and the dehydroxylating $In(OH)_3$.

4. Conclusions

In-ZSM-5 catalysts for the selective catalytic reduction of NO by methane are effectively promoted by extrazeolite CeO_2. The best results were achieved by adding the promoter as a high-surface-area CeO_2 powder (e.g., $X(NO) > 70\%$ at 100,000 h^{-1} between 723 and 773 K with 1000 ppm NO, 1000 ppm CH_4, and 2% O_2). Whereas the activity is strongly boosted in dry feed, the promotional effect is smaller in moist feed where appreciable NO conversions are achieved only at high temperatures.

During thermal stress, the CeO_2 promoter undergoes interactions with the zeolite component by which part of the Ce ions are stabilized in the +3 state in oxidative atmosphere. The majority of Ce ions remain, however, in the CeO_2 lattice. From the fact that the promotional effect is also observed with CeO_2 separated from the In-ZSM-5 into a layer preceding the zeolite, it can be concluded that the role of CeO_2 is to catalyze NO oxidation to provide a rich NO supply and that the CeO_2 acts independently from the other catalyst components.

It was observed that In-ZSM-5 catalysts with different active site structures exhibit different responses to promotion by ceria. Whereas intrazeolite indium oxo species, which are often considered the most important active sites in In-ZSM-5 SCR catalysts, are not among the most favorable cases upon promotion with CeO_2, the most intense promotional effects were found with sites that catalyze unselective methane oxidation in the absence of CeO_2 (intrazeolite InO_xCl_y species, extrazeolite In_2O_3 aggregates, probably active at the border with the zeolite). Similar activities were obtained with ternary mechanical mixtures of CeO_2, $In(OH)_3$, and NH_4-ZSM-5 provided that activation was performed in inert gas, whereas air calcination led to inferior performance. Evidence from TPR, FTIR, and XRD and from experiments with separate activation of mixture components led to the conclusion that the high activities observed are due to extrazeolite indium sites, which are probably at the border between In_2O_3 aggregates and external zeolite surface and may be engaged in In–O–Si and In–O–Al bridges.

The presence of acidic sites is another prerequisite for achieving NO reduction to N_2 over CeO_2-promoted In-

ZSM-5. The results obtained suggest that methane may be activated by In sites to be unselectively oxidized, or by NO_2 adsorbed on In sites to form a mobile intermediate containing both carbon and nitrogen, which enters a selective reaction path to N_2 over acidic sites. A rich supply of NO_2, as provided by the CeO_2 component, suppresses unselective methane oxidation also on those indium sites where it predominates at short NO supply.

Acknowledgments

Financial support by the Federal Ministry of Education, Science and Technology (BMBF), Grants 03C0271/B6 and 03C0271/A3, is gratefully acknowledged. We are also grateful to Rhodia Co. for donating high-surface-area CeO_2.

References

[1] M. Iwamoto, H. Yahiro, S. Shundo, Y. Yu-u, N. Mizuno, Shokubai 32 (1990) 430.
[2] M. Shelef, Chem. Rev. 95 (1995) 209.
[3] V.I. Parvulescu, P. Grange, B. Delmon, Catal. Today 46 (1998) 233.
[4] Y. Traa, B. Burger, J. Weitkamp, Micropor. Mesopor. Mater. 30 (1999) 3.
[5] D. Kaucky, A. Vondrova, J. Dedecek, B. Wichterlova, J. Catal. 194 (2000) 318.
[6] B. Wichterlova, J. Dedecek, Z. Tvaruzkova, Stud. Surf. Sci. Catal. 84 (1994) 1555.
[7] J. Sarkany, J.L. d'Itri, W.M.H. Sachtler, Catal. Lett. 16 (1992) 241.
[8] M. Iwamoto, H. Yahiro, N. Mizuno, W.-Z. Zhang, Y. Mine, H. Furukawa, S. Kagawa, J. Phys. Chem. 96 (1992) 9360.
[9] W. Grünert, N.W. Hayes, R.W. Joyner, E.S. Shpiro, M.R.H. Siddiqui, G.N. Baeva, J. Phys. Chem. 98 (1994) 10832.
[10] H.-Y. Chen, W.M.H. Sachtler, Catal. Today 42 (1998) 73.
[11] A.A. Battiston, J.H. Bitter, D.C. Koningsberger, Catal. Lett. 66 (2000) 75.
[12] F. Heinrich, C. Schmidt, E. Löffler, M. Menzel, W. Grünert, J. Catal. 212 (2002) 157.
[13] P. Marturano, L. Drozdova, A. Kogelbauer, R. Prins, J. Catal. 192 (2000) 236.
[14] R.W. Joyner, M. Stockenhuber, Catal. Lett. 45 (1998) 15.
[15] F. Heinrich, C. Schmidt, E. Löffler, W. Grünert, Catal. Commun. 3 (2001) 317.
[16] E. Kikuchi, K. Yogo, Catal. Today 22 (1994) 73.
[17] E. Kikuchi, M. Ogura, I. Terasaki, Y. Goto, J. Catal. 161 (1996) 465.
[18] M. Ogura, N. Aratani, E. Kikuchi, Stud. Surf. Sci. Catal. 105 (1997) 1593.
[19] X.J. Zhou, T. Zhang, Z.S. Xu, L.W. Lin, Catal. Lett. 40 (1996) 35.
[20] R. Heinisch, M. Jahn, C. Yallamas, Chem. Eng. Technol. 22 (1999) 337.
[21] T. Sowade, C. Schmidt, F.-W. Schütze, H. Berndt, W. Grünert, J. Catal. 214 (2003) 100.
[22] E. Kikuchi, M. Ogura, N. Aratani, Y. Sugiura, S. Hiromoto, K. Yogo, Catal. Today 27 (1996) 35.
[23] M. Ogura, M. Hayashi, E. Kikuchi, Catal. Today 42 (1998) 159.
[24] M. Ogura, M. Hayashi, E. Kikuchi, Catal. Today 45 (1998) 139.
[25] F.-W. Schütze, H. Berndt, T. Liese, T. Sowade, W. Grünert, F. Simon, U. Ströder, DP 10065717.6, December 22, 2000.
[26] F.-W. Schütze, H. Berndt, M. Richter, B. Lücke, C. Schmidt, T. Sowade, W. Grünert, Stud. Surf. Sci. Catal. 135 (2001) A10-O-1.
[27] H. Berndt, F.-W. Schütze, M. Richter, T. Sowade, W. Grünert, Appl. Catal. B: Environ. 40 (2003) 51.
[28] M. Ogura, T. Ohsaki, E. Kikuchi, Micropor. Mesopor. Mater. 32 (1998) 533.
[29] C. Schmidt, T. Sowade, E. Löffler, A. Birkner, W. Grünert, J. Phys. Chem. B 106 (2002) 4085.
[30] V. Kanazirev, V. Valtchev, M.P. Tarassov, Chem. Commun. (1994) 1043.
[31] M.R. Mihályi, H.K. Beyer, Chem. Commun. (2001) 2242.
[32] C. Schmidt, T. Sowade, F.-W. Schütze, M. Richter, H. Berndt, W. Grünert, Stud. Surf. Sci. Catal. 135 (2001) 30-P-15.
[33] R.M. Mihályi, G. Pál-Borbély, H.K. Beyer, C. Minchev, Y. Neinska, H.G. Karge, React. Kinet. Catal. Lett. 60 (1997) 195.
[34] D.C. Koningsberger, R. Prins, in: J.D. Winefordner (Ed.), Chemical Analysis, vol. 92, Wiley, New York, 1988, p. 673.
[35] F.-W. Lytle, D.E. Sayers, E.A. Stern, Physica B 158 (1989) 701.
[36] T. Ressler, J. Phys. IV France 7 (1997) C2–269.
[37] T. Sowade, Ph.D. thesis, Ruhr-Universität Bochum, 2002.
[38] A. Shichi, A. Satsuma, M. Iwase, K. Shimizu, S. Komai, T. Hattori, Appl. Catal. B 17 (1998) 108.
[39] T. Liese, Ph.D. thesis, Ruhr-Universität Bochum, 1999.
[40] M. Romeo, K. Bak, J. Elfallah, F. Lenormand, L. Hilaire, Surf. Interface Anal. 20 (1993) 508.
[41] S. Damyanova, C.A. Perez, M. Schmal, J.M.C. Bueno, Appl. Catal. A 234 (2002) 271.
[42] C. Schmidt, T. Sowade, W. Grünert, unpublished results.
[43] T. Liese, D. Rutenbeck, W. Grünert, in: M.M.J. Treacy, B.K. Marcus, M.E. Bisher, J.B. Higgins (Eds.), Proceedings of the 12th International Zeolite Conference, Materials Research Society, Baltimore, USA, 1998, p. 2795.